Physical Modeling Studies of Electrolyte Flow Due to Gas Evolution and Some Aspects of Bubble Behavior in Advanced Hall Cells: Part I. Flow in Cells with a Flat Anode

R. SHEKHAR and J.W. EVANS

The need for energy reduction in the electrolytic production of aluminum led to the concept of advanced Hall cells that can be operated at lower interelectrode gaps compared to existing cells. However, gas bubbles generated by the anodic reaction increase the resistivity of electrolyte and cancel out part of the reduction in interelectrode resistance expected from bringing the electrodes closer together. Therefore, the primary objective of this work was to determine a cell design in which flow can be managed to promote the removal of anode gas bubbles from the interelectrode gap. In particular, this article focuses on advanced Hall cells equipped with "flat" anodes, similar to those used in existing cells. The principal experimental tool has been a "water" model consisting of a large tank in which simulated anodes can be suspended in either the horizontal or near-horizontal configurations. Gas was generated by forcing compressed air through porous graphite, and the fine bubbles characteristic of inert anodes used in advanced Hall cells were produced by adding butanol to water. Velocities were measured using a laser-Doppler velocimeter (LDV). This study indicates that the existing cell configuration might not be the optimum configuration for advanced Hall cells. The results also show that operation of an advanced Hall cell with a fully submerged anode should give rise to higher electrolyte velocities and thus rapid removal of bubbles. The bubble effect should be further lowered in a near-horizontal configuration; however, the flow pattern could have an adverse effect on current efficiency and alumina distribution in the cell. It has also been shown that the bubble size, and, therefore, the physical properties of the electrolyte, can have a significant effect on the electrolyte flow pattern in the interelectrode gap.

I. INTRODUCTION

THE electrolytic production of aluminum in Hall-Héroult cells is an energy-intensive process accounting for nearly 4 pct of the electrical energy generated in the United States. High electrical energy costs provide great incentive for the minimization of this energy consumption. Reduction in energy consumption can be achieved in two ways: improvements in current efficiency and reduction in cell voltage. The latter has the greater potential, since efficiencies in modern cells exceed 94 pct, while actual cell voltages exceed the thermodynamic minimum of 1.75 V by a factor of over 2.

Figure 1 is a schematic (side) view of a typical Hall cell. Here current of the order of 150 kA is passed through the anode bus structure into the cryolite bath. Cryolite is a solvent for alumina fed to the cell. Carbon anodes, either prebaked or Soderberg (monolithic blocks of carbon baked from carbon paste within the cell), dip into the cryolite. Beneath the cryolite is a layer of molten aluminum. The cathodic reaction, that is, the reduction of aluminum ions, occurs at the interface between the two liquids.

The largest single part of the cell voltage is the drop of about 1.8 V caused by passage of current through the electrolyte-filled gap between the carbon anode and the metal pool which is the cathode. This anode-to-cathode distance (ACD) is 4 to 5 cm in present-day cells. Reducing this ACD, for the purpose of decreasing energy consumption, is not performed in practice because of the danger of shorting the cell through contact between the anodes and the metal pool. Shorting could occur in industrial cells because of (a) uncertainty concerning the position of the bottom of the consumable carbon anode, and (b) variation in the position of the metal/electrolyte interface under the influence of electromagnetic forces.

The need to reduce ACD has led to the concept of advanced Hall cells that use inert anodes (to replace the consumable carbon anodes presently being used) and wettable refractory cathodes (on which a thin film of aluminum will form rather than the pool of aluminum in existing cells). In recent years, most of the work on advanced Hall cells has been devoted to research and development of materials for the inert anode[7] and refractory cathode.[2,3] There is a reasonable expectation that these materials will become available during this decade, and the question of how a cell is to be designed using them must be addressed. Unfortunately, very little attention has been paid to the operational aspects of advanced Hall cells. These aspects will be the subject of this article.

II. PREVIOUS INVESTIGATIONS

The most significant work pertaining to the operation of an advanced Hall cell was carried out by Dorward.[1]

R. SHEKHAR, Assistant Professor, is with the Department of Metallurgical Engineering, Indian Institute of Technology, Kanpur 208 016, India. J.W. EVANS, Professor, is with the Department of Materials Science and Mineral Engineering, University of California, Berkeley, CA 94720.

Manuscript submitted June 25, 1992.

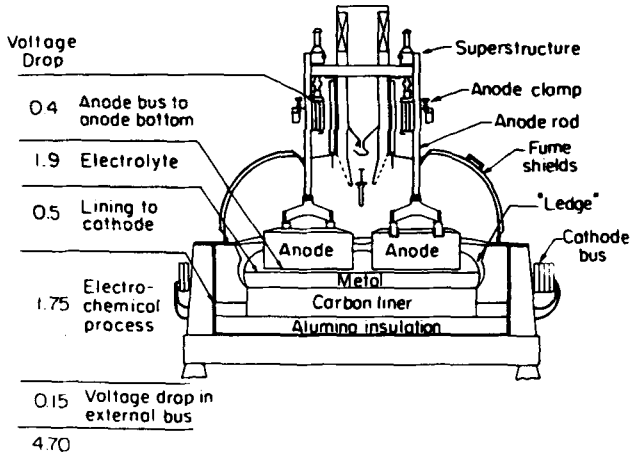

Fig. 1—A typical Hall cell with voltage drop across various parts. From Ref. 13. (A modern cell would typically have a somewhat lower total voltage.)

He showed that the voltage drop across the gap between the anode and cathode was not proportional to the ACD; as the ACD was reduced, the cell voltage decreased by less than the amount anticipated. This phenomenon, hereafter called the "bubble effect," was because of gas bubbles, generated by the anodic reaction, in the anode-to-cathode gap (ACG). As the ACD was reduced, these bubbles occupied a greater fraction of the electrolyte volume in the ACG, thereby increasing the resistivity of the electrolyte. This canceled out part of the expected reduction in interpolar resistance on bringing the electrodes closer.

Dorward and Payne[2] reported on a study of the bubble effect in a water model of an advanced Hall cell. They used a rectangular plastic tank, 1 × 1.5 × 1-m deep, that contained a simulated anode, which consisted of 18 porous brass plates through which air could be passed at a controlled rate to simulate the gas generated at the anode at various current densities. The cathode consisted of an array of copper bars inset into a LUCITE* plate to produce a smooth surface. Provision was also made for tilting the electrodes from the horizontal (while maintaining them parallel). The electrolyte was simulated by a dilute potassium chloride solution, and the interpolar resistances were determined by passing alternating current at set voltage and measuring the electrical current. In this way, the variation of interpolar resistance from plate to plate across the anode could be studied. Dorward and Payne observed that, for electrodes inclined to the horizontal, the resistance increased toward the upper side of the ACG, which is to be expected because this is the direction of bubble travel and, therefore, increasing (simulated) gas fraction. The overall interpolar resistance increased with increasing current density and increased with decreasing electrode inclination from the horizontal, particularly up to inclinations of 4 deg. In an earlier study,[3] a slight reduction in interpolar resistance was also obtained when a near-vertical electrode configuration was used.

*LUCITE is a trademark of the Clorox Company, Oakland, CA.

The previously mentioned experiments suggest that the horizontal electrode configuration used in existing cells might not be the optimum configuration in terms of bubble effect and, therefore, energy consumption. Clearly, any novel cell design should be such that the anode gas bubbles are rapidly removed from the ACG.

The dynamics of bubble flow in Hall cells are complex; both electromagnetic forces and bubble buoyancy effects cause flow of bath. The bubbles are, in turn, affected by the flow; faster-flowing electrolyte reduces the residence time of bubbles in the ACG. Because bubble and electrolyte flow in the ACG are inter-related, analysis of an advanced Hall cell would be incomplete without a knowledge of the flow field in the ACG. There is also a need to systematically study and compare the electrolyte flows in the different electrode configurations, namely, horizontal, near-horizontal, and near-vertical. The importance of electrolyte flow cannot be underestimated since it also affects the dissolution and distribution of alumina, deterioration of the electrodes, and heat transfer at the ledge-electrolyte interface.

Studies thus far on the nature of electrolyte flow have been very few,[4,5,6] and they do not characterize flow in the ACG in sufficient detail. Moreover, these studies have been confined to the simulation of existing cells,[9] and the effect of parameters which might influence bubble effect, such as electrode configuration and anode design, have not been investigated.

Hall cells are capital intensive, and therefore, efforts should be made to retrofit existing cells. Hence, the objective of this study has been to suggest design and operating conditions which promote the rapid removal of bubbles from the ACG and thereby minimize bubble effect in an advanced Hall cell. These conditions should be such that they can be implemented in existing cells without significant modifications. Moreover, because of the difficulties in measuring electrolyte velocities in industrial cells, data collected from this work can be used to test mathematical models for the purpose of scale-up and design. The methodology used in this work entailed the detailed characterization of electrolyte flow and interpolar resistance in the ACG as a function of design and operating parameters such as electrode configuration, anode design, and current density. Bubbles are not the only cause of electrolyte motion in Hall cells. Electromagnetic forces[11] and natural convection also cause motion. It has long been recognized that electromagnetic forces are a major cause of flow within the cell, and mathematical models (*e.g.*, Reference 12) permit such electromagnetic forces to be calculated. They are of the order of 50 N/m^3. The component of the buoyancy force resulting from bubbles in the ACG in the steepest direction parallel to the anode face would be $\rho\ \phi\ g \sin\theta$, where ρ is the electrolyte density, ϕ the gas fraction in the ACG, g the gravitational acceleration, and θ the anode inclination to the horizontal. Substitution of realistic values for these parameters yields buoyancy forces of a few hundred N/m^3. Consequently, within the ACG, buoyancy effects resulting from gas bubbles are dominant, while outside the ACG, electromagnetic forces will play a more significant role. Results pertaining to velocity measurements with a flat anode will be presented in this article. Part II, a companion article,

will contain flow and interpolar resistance measurements in a new "grooved" anode arrangement.

III. EXPERIMENTAL APPARATUS

Figure 2 is a schematic diagram of an industrial Hall cell viewed (a) from above and (b) looking in a direction parallel to the long dimension of the cell. In these figures, 2A is the width of the center channel, 2B the distance between adjacent anodes (inter-anode gap), and C the anode-sidewall (ledge) distance. It is apparent from Figure 2(a) that flow in the vicinity of one anode, say anode number 8, is symmetric about a vertical plane passing through its center. That is, flow in the region shown by dashed lines in Figures 2(a) and (b) should be approximately representative of flow in the vicinity of all anodes, except those which are adjacent to the (shorter) side walls of the cell, that is, anode numbers 1, 10, 5, and 6.

The physical model entailed simulation of bubble-driven flow in the ACG of an isolated, industrial-size anode-cathode arrangement. Because of the high current requirements, anodic gas bubbles were not produced electrolytically. Instead, bubbles were generated by passing compressed air through a porous graphite plate.

A. *Electrolyte Selection*

Because the physical model is geometrically similar to an industrial Hall cell, the key concern was selection of the simulated electrolyte to provide similarity between the gas-driven buoyancy forces of the physical model and those in a Hall cell. Other important requirements for the simulated electrolyte were that they should (a) not be hazardous, (b) be transparent to facilitate measurements with a laser-Doppler velocimeter (LDV), (c) be compatible with the construction material of the physical model, namely acrylic polymer, and (d) be easily available.

Based on the previously mentioned criteria, a water-0.5 vol pct butanol mixture was used as "electrolyte" for the physical model. Table I compares the relevant properties and dimensionless numbers for the industrial electrolyte (cryolite), water-butanol mixture, and tap water. Bubble sizes in cryolite for advanced Hall cells were reported in the literature,[1] whereas those in tap water and water-butanol mixtures were measured using a smaller version of the anode described in Section B.[10] The bubble Reynolds number (ReI), terminal velocity, and bubble shape were estimated using the graphical correlation of Grace.[8]

Inspection of the Navier-Stokes equations shows that identical velocities can be expected in a physical model when the geometries of the model and the real system are identical, the kinematic viscosities are the same, and the forces per unit volume of fluid are the same. The geometry of the physical model matches that of a real cell in both shapes and dimensions, except for some imperfection resulting from the baffles (Section B). From Table I, it is seen that the kinematic viscosities are well matched in the model fluid and the real electrolyte. The flow in the real cell and the flow in the model are driven by a buoyancy force which is a consequence of the apparent density difference between a liquid containing bubbles and one free of bubbles. Per unit volume, this force is proportional to $\phi(\rho_{(l)} - \rho_{(g)})/\rho_{(l)}$, where ϕ is the volume fraction of gas, $\rho_{(l)}$ is the liquid density, and $\rho_{(g)}$ is the gas density. To a good approximation, this quantity equals ϕ. Consequently, velocities in the real cell will be approximated by those in the physical model if the gas fraction ϕ is the same in the cell and in the model. There do not appear to have been any measurements of gas fraction in Hall cells with advanced electrodes, and gas fractions have not been measured in the present model. Gas bubbles are generated at the anode surface and move until they reach the free surface of the electrolyte. The gas fraction in the electrolyte is therefore dependent on the residence time as determined by the bubble motion and the geometry (as well as by the volumetric flow of gas, which is set equal in the model to that in the cell). Bubble motion is partly a convection of the bubble by the moving electrolyte and partly the motion of the bubble relative to the electrolyte. To a first approximation, the latter is likely to be similar in the model and in the cell if the bubble terminal velocities are similar. These terminal velocities are shown in the last column of Table I and are seen to be comparable in magnitude. That the terminal velocities in the real cell are lower than those in the physical model suggests that the model may underestimate the gas fraction and, therefore, the effects of bubbles. The Morton (Mo) and Eotvos (Eo) numbers appearing in Table I serve to characterize the shape and rise velocity of a bubble, and their influence on the bubble-driven flow is indirect (through the influence of bubble size on gas fraction).

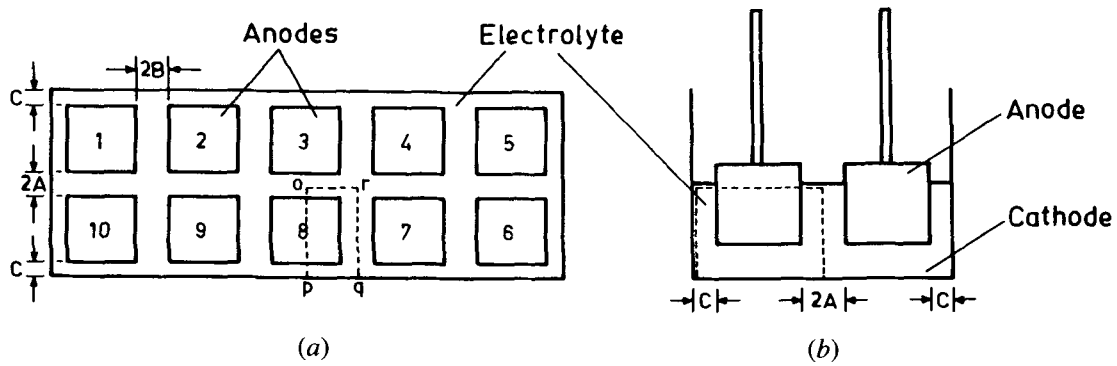

Fig. 2—Schematic diagram of an industrial Hall cell viewed from (*a*) above and (*b*) across the shorter cell dimension.

Table I. Properties and Dimensionless Numbers for Industrial Electrolyte (Cryolite), Water-Butanol Mixture, and Tap Water

	σ (n/m)	μ (kg/ms)	ρ (kg/m^3)	ν (m^2/s)
Cryolite	0.5	0.003	2100	1.4×10^{-6}
Water-0.5 pct butanol	0.062	0.001	1000	10^{-6}
Water	0.072	0.001	1000	10^{-6}

	d_b (mm)	Mo	Eo	Re_b	Bubble Shape	Bubble Terminal Velocity (m/s)
Cryolite	0.1 to 0.5	3.02×10^{-12}	0.01	30	spherical	0.084
Water −0.5 pct butanol	1.0	4.1×10^{-11}	0.16	200	spherical	0.2
Water	1 to 3	2.5×10^{-11}	1.3	1000	ellipsoid	0.33

Note: Dimensionless numbers shown for larger bubbles.

B. *Physical Model*

Figure 3 is a view of the laboratory tank (152 × 89 × 92-cm high) seen from above with an anode in position along with two baffles. The coordinate system used in this investigation is also shown in Figure 3. The origin is on the face of the anode at one of its two lower corners. The Z coordinate is positive upward. One baffle is placed directly against the left of the anode, while the second baffle is positioned directly below the anode (in the figure). This arrangement ensures that the physical model will approximately simulate flow in the region shown by the dashed lines in Figure 2. The baffle along the line k-l and the sides of the tank parallel to the lines i-j and i-l prevent flow through the planes they occupy, which are symmetry planes in the actual cell and, therefore, experience no transverse flow. However, the baffle and walls will exert a drag on the moving electrolyte, whereas the corresponding planes in the real cell, not being real surfaces, will not. The model is, therefore, imperfect, and velocities close to the baffle and walls will not be realistic. However, the contact area between the baffle or walls and the electrolyte is small, compared to the contact area of the simulated anode and cathode. Consequently, the imperfect simulation is likely to have little effect throughout most of the model, particularly in the ACG. The values of A, B, and C used in the physical model are typical of those found in industrial Hall cells. Figure 4 is a side view of the physical model, showing some of the important parameters used in these experiments, such as ACD, ACG, and submergence. Here submergence refers to the height of the (simulated) electrolyte above the highest point of the anode top. Therefore, a negative submergence implies that part of the anode is protruding above the electrolyte surface, the usual arrangement for Hall cells but one that may not be necessary for advanced cells.

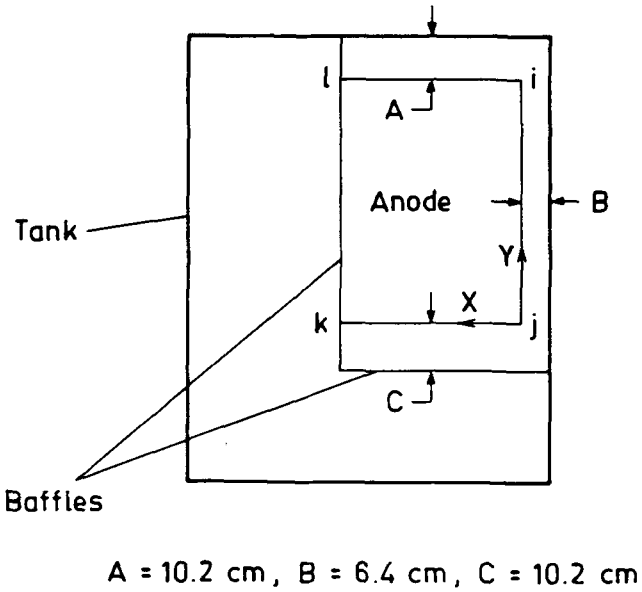

Fig. 3—Top view of the experimental apparatus showing the tank and the anode.

The anode consisted of a 6.5-mm-thick graphite plate (30.8 × 90.2 cm) that was fastened to a 12.5-mm-thick acrylic plate. The graphite was permeable (0.1 darcys). Inert anodes can be considerably thinner than conventional prebaked anodes since they are not consumed during the anodic reaction. Several slots, 9.6-mm wide and 3.2-mm deep, were made in the acrylic plate. Air was supplied to the anode through hose fittings placed at the center of each slot. Each slot was connected to a separate flow meter to ensure uniform air supply throughout the entire face of the graphite. To guard against leaks, a rubber gasket was placed between the graphite slab and the acrylic plate. The anode was suspended with the help of four aluminum rods that were attached to the acrylic plate. Provision was also made to tilt the anode from the horizontal position. The top surface of an acrylic box represented the cathode. In all experiments, the cathode was placed parallel to the anode.

C. *Velocity Measurements*

Velocities were measured with an LDV. The LDV consisted of a 35-mW He-Ne laser and optics such as the beam splitter, photomultiplier, and beam expander and a 750-mm transmitting lens. The LDV was operated in the dual-beam, backscattered mode. A frequency shifter (Bragg cell) was used to resolve directional ambiguity and reduce the error caused by fringe bias. Doppler signals were processed by a TSI counter, interfaced with an APPLE II PLUS* microcomputer for data acquisition

*APPLE II PLUS is a trademark of Apple Computer, Inc., Cupertino, CA.

and storage. Further, the LDV was operated in the total burst mode (with a minimum of eight cycles) to overcome the problem of velocity bias.

Operation of the LDV was validated by measuring axial velocities in a 0.9-m-tall pipe, 0.063 m in diameter, through which water was passed at a flowrate of 1.67×10^{-4} m^3/s. The calculated flowrate, using axial velocities measured at various radial positions, was similar to the observed value. Moreover, before velocities were measured in the physical model, reproducibility tests were conducted. These tests showed that both the time-averaged and fluctuating velocities (a measure of turbulence) were reproducible.[10]

Because the LDV, positioned to the right in Figure 3, is only capable of measuring velocity components perpendicular to its optical axis, flow in the Y and Z directions can be measured, but not in the X direction. Z-direction velocities could be measured in the ACG only close to $X = 0$ (Figure 3) because the laser beams would be obstructed by the (simulated) electrodes. In any case, Z-direction velocities were expected to be small. Consequently, in all the plots depicting flow in the ACG, only Y-direction velocities appear, although it can be inferred that X-direction velocities are significant in some cases.

All the experiments reported in this article have been carried out at an air flow rate corresponding to a current density of 0.9 A/cm^2, which is close to the value employed in industrial Hall-Héroult cells. For advanced Hall cells, where oxygen is evolved at the anode, this current density corresponds to an air flow rate of 0.225 cm^3/s per cm^2 of anode area (1233 K, atmospheric pressure). Experimental results have been presented in the form of vector plots which represent the flow pattern in a plane parallel to the electrodes and passing through the center of the ACG. Velocity measurements were also carried out at two representative locations (Y = 14 and 75 cm) to characterize the velocity profile across the ACG.

IV. RESULTS AND DISCUSSION

Because of the high costs involved in drastically modifying existing Hall cells, there would be a tendency to operate an advanced Hall cell with the same configuration that is used in a conventional Hall cell. That is, the cell would be operated with horizontal electrodes and negative submergence. The resulting electrolyte flow pattern is presented in Figure 5. It appears from this figure that electrolyte velocities in the center of the ACG are of the order of only 3 cm/s, with velocities across the ACG being similar.[10] Consequently, to obtain higher electrolyte velocities, other configurations for Hall cells must be examined.

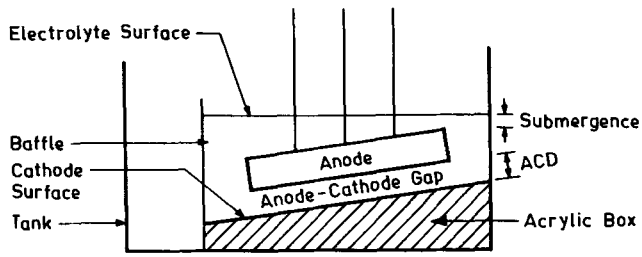

Fig. 4—Side view of the experimental apparatus for (*a*) horizontal and (*b*) near-horizontal electrodes.

A. *Effect of Submergence*

One such configuration would be to operate a Hall cell with fully submerged anodes. Clearly, this scenario would not be possible in a conventional cell, where the electrolyte would corrode the iron rods supporting the anodes. However, in an advanced Hall cell, the support rods can be enclosed in hollow tubes made of the same material as the inert anode. Increasing the submergence to 2.5 cm in the configuration corresponding to Figure 5 leads to considerably higher velocities, as shown in Figure 6. Velocity measurements also show that flow is roughly uniform in the lower half of the ACG.[10] Measurements close to the anode were precluded by the presence of a 4- to 6-mm-thick bubble layer adjacent to the anode. Furthermore, velocity measurements showed considerable upflow in the interanode gap, that is, in the channel represented by B in Figure 3. This was consistent with the visual observation that a majority of the bubbles flowed out into the interanode gap (in the absence of any significant buoyancy force in the Y direction).

Based on the previously mentioned information, the nature of electrolyte flow in this configuration can be described. Here the electrolyte flows out of the ACG into the interanode gap, where it moves in the upward

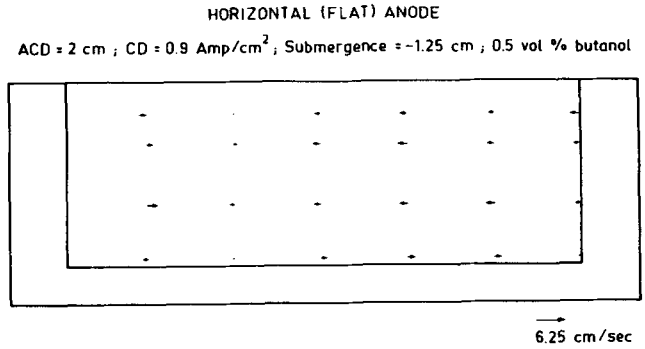

Fig. 5—Electrolyte flow in a simulated advanced Hall cell with a configuration similar to a conventional Hall cell (ACD = 2 cm, submergence = −1.25 cm, 0.5 vol pct butanol).

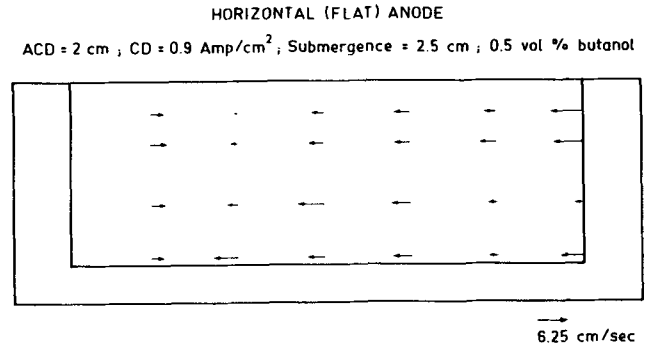

Fig. 6—Effect of submergence on flow in an advanced Hall cell when compared to Fig. 5.

direction and then goes over the top of the anode. Here it splits into two opposite directions along the length of the anode: one part flows toward the center channel and enters the ACG below edge il in Figure 3, while the other enters the ACG from the opposite end, that is, the gap between the anode and the ledge (edge jk in Figure 3).

B. *Effect of Near-Horizontal Electrode Orientation*

The second configuration that warrants close inspection is the near-horizontal electrode configuration. One difference between the present configuration and that of Dorward and Payne[2] was that the present anode was completely submerged in the (simulated) electrolyte; *i.e.*, the anode face is slightly inclined to the horizontal. It was believed that a cell with a submerged anode, where the return flow path of the electrolyte is above the anode top, would provide higher electrolyte velocities. This view was justified by experiments in the horizontal electrode configuration that were described in Section III–A.

Inclining the electrodes at an angle of 11.1 deg from the horizontal resulted in a nonuniform electrolyte flow pattern as shown in Figures 7 and 8. A schematic diagram of this flow is shown in Figure 9. It is seen from Figure 8 that electrolyte flow near the anode is unidirectional, that is, from the lower to the higher end of the ACG, with velocities of the order of 10 cm/s as the upper end of the ACG is approached. On the other hand, velocity in the vicinity of the cathode decreases, and even reverses direction (shown by negative values in Figure 8) as the higher end of the ACG is approached. Here the bubble layer was also much thinner than the 4- to 6-mm-thick layer observed in the corresponding horizontal configuration. Therefore, it can be said with reasonable certainty that inclining the electrodes from the horizontal configuration would reduce the bubble effect because of the higher electrolyte velocities near the anode which would sweep the gas bubbles more rapidly out of the ACG. However, the flow reversal in the lower half of the ACG could bring some oxygen bubbles into contact with aluminum, leading to its reoxidation, with the consequent reduction in current efficiency of the cell.

C. *Effect of Physical Property of the Electrolyte*

The effect of physical property of the electrolyte on the flow pattern was investigated by varying the butanol concentration in tap water. In these experiments (Figure 10), the electrolyte was tap water, the surface tension of which is 0.072 N/m, compared to 0.062 N/m for the water-0.5 pct butanol mixture used in earlier experiments.

Clearly, the absence of butanol results in a more rapidly flowing electrolyte that is essentially unidirectional,

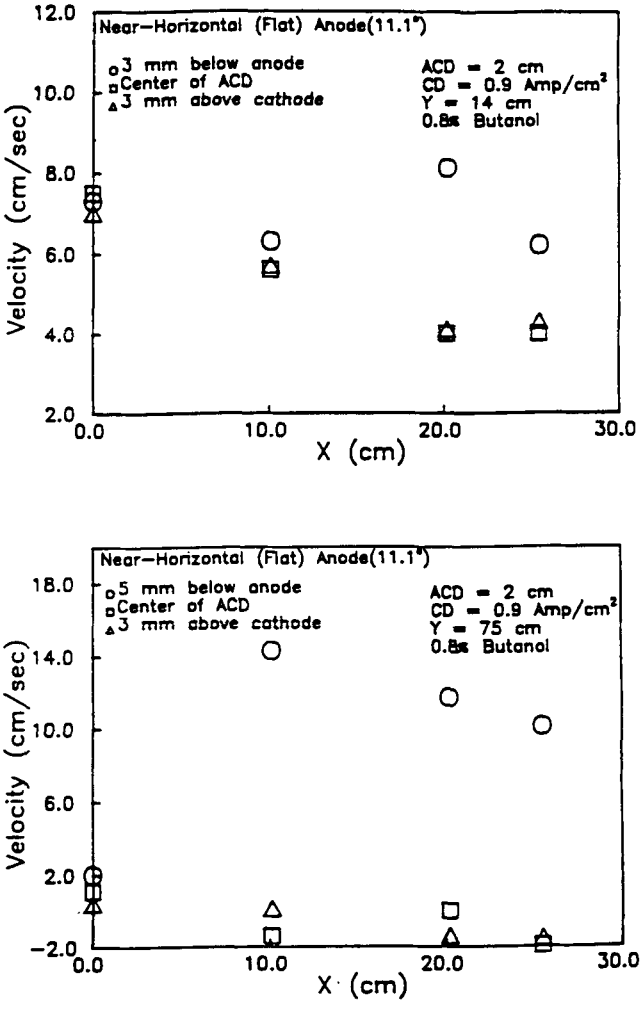

Fig. 8—Electrolyte flow pattern across the ACG in a configuration corresponding to Fig. 7.

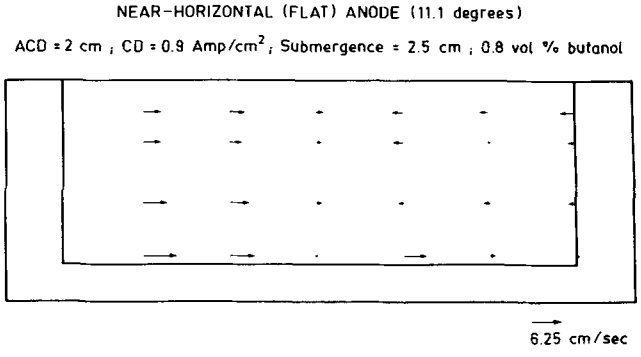

Fig. 7—Effect of electrode inclination on flow in an advanced Hall cell when compared to Fig. 6.

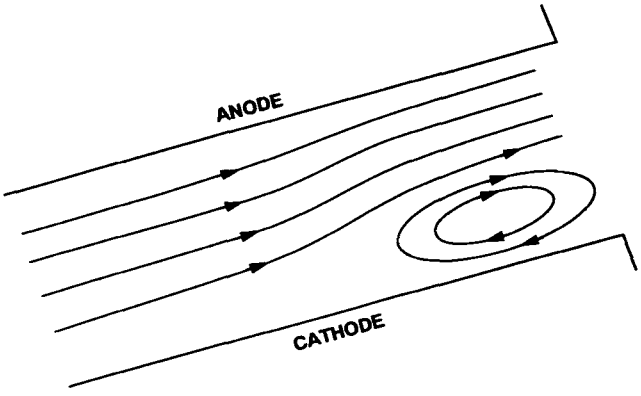

Fig. 9—Schematic diagram of flow in the ACG for a configuration corresponding to Fig. 7.

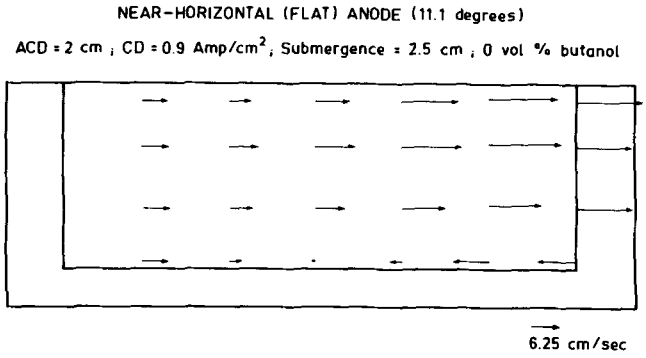

Fig. 10—Effect of butanol concentration on electrolyte flow when compared to Fig. 7.

with maximum velocities reaching 22 cm/s near the anode, although the direction of flow is similar to that observed in Figures 7 and 8. The effect of surface tension or butanol concentration on the flow pattern can be explained as follows. Very small bubbles were generated in the presence of butanol, and a large fraction was observed to flow into the interanode gap (channel B in Figure 2), generating considerable flow in the $-X$ direction, at the expense of flow in the Y direction. However, in the configuration corresponding to Figures 10 and 11, the larger-size bubbles move predominantly along the length of the anode, in the $+Y$ direction, resulting in higher electrolyte velocities parallel to the electrodes. This line of reasoning was verified by vertical velocity measurements in the interanode gap, which showed considerable upflow for the configuration corresponding to Figures 7 and 8.[10] In contrast to the above observations, experiments in the horizontal electrode configuration showed that butanol concentration did not have a very significant effect on the flow pattern.[10]

The experiments in this section therefore point to the possibility of manipulating electrolyte flow by changing those properties of the electrolyte that have a bearing on bubble size. Furthermore, they also suggest that characterizing flow in the ACG with average velocity measurements at one or two locations may lead to erroneous conclusions.

V. CONCLUSIONS

This study suggests that the horizontal electrode configuration used in existing cells might not be the optimum configuration for advanced Hall cells in terms of bubble effect and, therefore, energy consumption. It also sheds some light on the operation of an advanced Hall cell as follows:

1. Operation of an advanced Hall cell with a submerged anode should give rise to higher electrolyte velocities and, thus, reduced bubble effect.
2. Bubble effect should be further lowered in a configuration where the anode is slightly tilted from the horizontal (with a submerged anode) because of the comparatively high electrolyte velocities near the anode. Unfortunately, the nonuniform flow pattern in this configuration could lead to adverse effects such as reoxidation of aluminum and nonuniform concentration of alumina in the ACG.
3. It was also observed that the physical properties of the electrolyte can have a significant effect on the electrolyte flow pattern, the effect being opposite for the horizontal and near-horizontal configurations. That is, flow in the ACG can be manipulated by modifying, for example, the surface tension of the electrolyte.

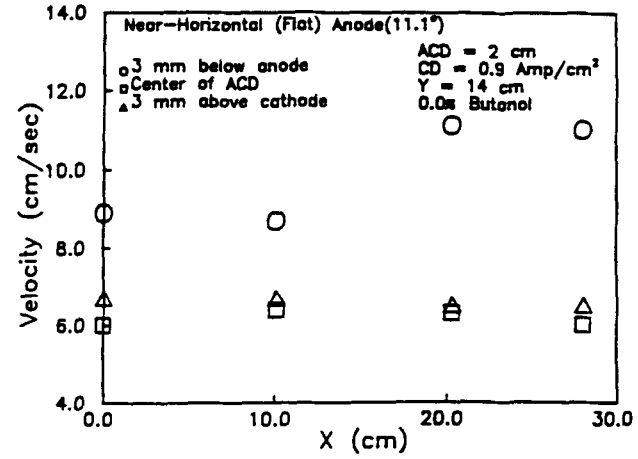

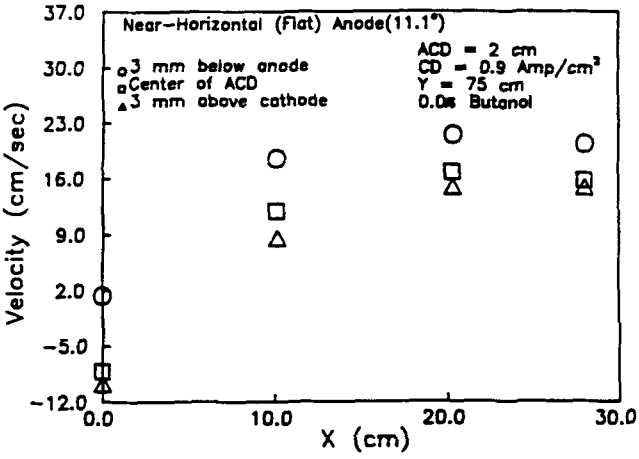

Fig. 11—Electrolyte velocities across the ACG in a configuration corresponding to Fig. 10.

Because inert anodes are not consumed during the electrolytic reaction, unlike the conventional carbon anodes, anode design could be an important parameter in reducing bubble effect. Moreover, electrolyte flow measurements by themselves are not sufficient; interpolar resistance measurements are essential to characterize bubble effect. This will be the subject of Part II, a companion article, intended to demonstrate the importance of anode design in determining the energy efficiency of advanced Hall cells.

NOMENCLATURE

A	half the width of the center channel
ACD	anode-to-cathode distance
ACG	anode-to-cathode gap

B	half the interanode gap
C	anode-sidewall distance
d	diameter
Eo	Eotvos number $(gd_b^2(\rho_e - \rho_g)/\sigma)$
g	acceleration due to gravity
Mo	Morton number $(g\mu_e^4/\rho_e\sigma^3)$
Re_b	bubble Reynolds number $(\rho_e d_b u/\mu_e)$, where u is the bubble terminal velocity
X	horizontal direction parallel to the long side of the cell
Y	horizontal/near-horizontal direction parallel to the short side of the cell
Z	vertically upward direction
μ	viscosity (kg/m s)
ϕ	gas fraction in ACG
σ	surface tension (N/m)
ν	kinematic viscosity (m^2/s)
θ	inclination of anode to horizontal
ρ	density (kg/m^3)

Subscripts

b	bubble
c	cryolite
e	electrolyte
g	gas
l	liquid

ACKNOWLEDGMENTS

The authors are grateful to the Department of Energy, which provided financial assistance for this project under Subcontract No. C87-101226-002. Dr. Matt McMonigle of DOE, Dr. J.V. Anderson of EG&G Idaho, Dr. John Payne of Kaiser Aluminum, and Dr. Nolan Richards of Reynolds Aluminum provided useful suggestions for the design of the anodes and the experiments. We are also thankful to Joe Waidl, Ken Yee, and Charles Brown for the construction of the experimental apparatus and to Felipe Franco for assisting with the velocity measurements.

REFERENCES

1. R.C. Dorward: *J. Appl. Electrochem.*, 1982, vol. 13, p. 569.
2. R.C. Dorward and J.R. Payne: *An Evaluation of a Titanium Diboride Composite Material as Cathode for Low Energy Alumina Reduction Cells*, Topical Report DOE/CS/40215-2, Kaiser Aluminum and Chemical Corp., Oakland, CA, 1985.
3. R.C. Dorward and J.R. Payne: *Development of Monolithic Titanium Diboride Cathodes for Retrofit Hall Cell Applications*, Report DOE, DE-AC07-76CS40215, Kaiser Aluminum and Chemical Corp., Oakland, CA, 30 June 1976–30 June 1983.
4. K. Grjotheim, C. Krohn, R. Naeumann, and K. Tørklep: *Metall. Trans.*, 1970, vol. 1, p. 3133-3141; 1971, vol. 2, pp. 199-204; 1973, vol. 4, pp. 1945-52.
5. E. Dernedde and E.L. Cambridge: *AIME Light Met.*, 1975, vol. 1, p. 111.
6. A. Solheim, S.T. Johansen, S. Rolseth, and J. Thonstad: *AIME Light Met.*, 1989, p. 245.
7. J.D. Weyand, S.P. Ray, F.W. Baker, D.H. DeYoung, and G.P. Tarcy: *Inert Anodes for Aluminum Smelting*, Final Report, DOE/CS/40158-20, ALCOA, Feb. 1986.
8. J.R. Grace: *Trans. Inst. Chem. Eng.*, 1973, vol. 51, p. 116.
9. S. Fortin, M. Gerhardt, and A.J. Gesing: *AIME Light Met.*, 1984, p. 721.
10. J.W. Evans and R. Shekhar: *Physical Modeling of Bubble Phenomena, Electrolyte Flow and Mass Transfer in Simulated Advanced Hall Cells*, Report to DOE and Addendum, Subcontract No. C87-101226-002, University of California, Berkeley, CA, 1990 (DOE-ID-10281 and DOE-ID-10281-ADD).
11. R. Moreau and J.W. Evans: *J. Electrochem. Soc.*, 1984, vol. 131, p. 2251.
12. S.D. Lympany and J.W. Evans: *Metall. Trans. B*, 1983, vol. 14B, pp. 63-70.
13. K. Grjotheim, R. Huglen, and H. Kvande: in *Understanding the Hall-Héroult Process for Production of Aluminum*, K. Grjotheim and H. Kvande, eds., Aluminium-Verlag, Düseldorf, 1986, p. 19.